Mst1/Mst2 Regulate Development and Function of Regulatory T Cells through Modulation of Foxo1/Foxo3 Stability in Autoimmune Disease

Xingrong Du,* Hao Shi,* Jiang Li,* Yongli Dong,* JieLiang Liang,* Jian Ye,* Shanshan Kong,* Shujing Zhang,* Tao Zhong,* Zengqiang Yuan,† Tian Xu,*,‡ Yuan Zhuang,*,§ Biao Zheng,¶ Jian-Guo Geng,‖ and Wufan Tao*

Foxp3 **expression and regulatory T cell (Treg) development are critical for maintaining dominant tolerance and preventing autoimmune diseases. Human** ***MST1*** **deficiency causes a novel primary immunodeficiency syndrome accompanied by autoimmune manifestations. However, the mechanism by which** ***Mst1*** **controls immune regulation is unknown. In this article, we report that** ***Mst1*** **regulates** ***Foxp3*** **expression and Treg development/function and inhibits autoimmunity through modulating Foxo1 and Foxo3 (Foxo1/3) stability. We have found that** ***Mst1*** **deficiency impairs** ***Foxp3*** **expression and Treg development and function in mice. Mechanistic studies reveal that Mst1 enhances Foxo1/3 stability directly by phosphorylating Foxo1/3 and indirectly by attenuating TCR-induced Akt activation in peripheral T cells. Our studies have also shown that** ***Mst1*** **deficiency does not affect Foxo1/3 cellular localization in CD4 T cells. In addition, we show that** ***Mst1*** $^{-/-}$ **mice are prone to autoimmune disease, and mutant phenotypes, such as overactivation of naive T cells, splenomegaly, and autoimmune pathological changes, are suppressed in** ***Mst1*** $^{-/-}$ **bone marrow chimera by cotransplanted** ***wt*** **Tregs. Finally, we demonstrate that** ***Mst1*** **and** ***Mst2*** **play a partially redundant role in Treg development and autoimmunity. Our findings not only identify Mst kinases as the long-searched-for factors that simultaneously activate Foxo1/3 and inhibit TCR-stimulated Akt downstream of TCR signaling to promote** ***Foxp3*** **expression and Treg development, but also shed new light on understanding and designing better therapeutic strategies for** ***MST1*** **deficiency–mediated human immunodeficiency syndrome.** ***The Journal of Immunology*****, 2014, 192: 1525–1535.**

Regulatory T cells (Tregs) play crucial roles in preserving immunological self-tolerance and immune homeostasis by suppressing aberrant or excessive immune responses, such as autoimmune diseases and allergies. Tregs express the signature forkhead family transcription factor Foxp3. Mutations in *Foxp3* and *FOXP3* lead to autoimmune disorders in Scurfy mice and in humans, respectively (1). Overexpression of *Foxp3* in peripheral $CD4^+$ $CD25^-$ T cells enhances the suppressive function and conversion of naive $CD4^+$ T cells to Tregs (2, 3). However, the molecular mechanisms underlying the regulation of *Foxp3* expression are not fully understood.

Foxo1 and Foxo3 (Foxo1/3) transcription factors are required for *Foxp3* expression and Treg development (4, 5). *Foxo1* $^{-/-}$*Foxo3* $^{-/-}$ mice have impaired Treg development and function and display severe autoimmune disorders (5, 6). Foxo1/3 activity is negatively regulated by Akt, which can phosphorylate Foxo1/3 and promote their nuclear export and degradation (7–9). Sustained Akt activity inhibits de novo *Foxp3* expression and Treg development (10, 11), probably through inactivation of Foxo1/3. PI3K–Akt signaling can be stimulated by TCR and is required for the survival and homeostasis of T cells (12). However, *Foxp3* expression and Treg development also require TCR/CD28 stimulation. Therefore, in developing T cells, Akt activity has to be maintained at a proper level that is low enough to guarantee Foxo1/3 activity to promote Foxp3 expression and Treg differentiation, but high enough to ensure T cell survival. Such a factor or factors acting downstream of TCR signaling to specifically attenuate Akt activity have not yet been identified.

Mst1 and *Mst2* (*Mst1/2*) are two mammalian homologs of *Drosophila hpo* encoding a Ser/Thr kinase (13). *Mst1* $^{-/-}$*Mst2* $^{-/-}$ mice develop spontaneous tumors in liver, colon, and ethyl-*N*-nitrosourea–induced lymphomas/leukemias (14–18). Mst1 induces apoptosis through caspase-mediated proteolytic activation and histone H2B phosphorylation (19), or by enhancing Foxo1/3 nuclear entry through phosphorylation of Foxo1 and Foxo3 at S212 and S207, respectively, in fibroblasts and granule neurons (20, 21). Mst1/2 proteins may also promote apoptosis by interacting and suppressing Akt activation in

*State Key Laboratory of Genetic Engineering and Institute of Developmental Biology and Molecular Medicine, National Center for International Research of Development and Diseases, School of Life Sciences, Fudan University, Shanghai 200433, China; †Institute of Biophysics, Chinese Academy of Sciences, Beijing 100101, China; ‡Howard Hughes Medical Institute, Department of Genetics, Yale University School of Medicine, New Haven, CT 06536; §Department of Immunology, Duke University Medical Center, Durham, NC 27701; ¶Department of Immunology, Baylor College of Medicine, Houston, TX 77030; and ‖Biologic and Materials Sciences, University of Michigan School of Dentistry, Ann Arbor, MI 48109

Received for publication April 22, 2013. Accepted for publication December 2, 2013.

This work was supported by the National Basic Research Program of China (Grants 2013CB945300, 2011CB510102, and 2006CB806700); the National Natural Science Foundation of China (Grants 31171406, 30971666, and 30630043); the High Technology Research and Development Program of China (Grant 2007AA022101); and the Key Projects Grant for Basic Research (Grant 12JC1400600) from the Science and Technology Committee of Shanghai Municipality.

X.D., Y.D., and W.T. designed research; X.D., H.S., J. Li, Y.D., J.L. Liang, J.Y., S.K., and S.Z. performed research, data collection and statistical analysis; T.Z., Z.Y., B.Z., J.-G.G., and T.X. contributed vital new reagents or analytical tools; X.D., H.S., J. Li, Y.D., B.Z., Y.Z., J.-G.G., and W.T. analyzed and interpreted data; and X.D., Y.D., and W.T. wrote the manuscript.

Address correspondence and reprint requests to Dr. Wufan Tao and Dr. Yongli Dong, Institute of Developmental Biology and Molecular Medicine, Fudan University, 220 Handan Road, Shanghai 200433, China. E-mail addresses: wufan_tao@fudan.edu.cn (W.T.) and yongli_dong@fudan.edu.cn (Y.D.)

The online version of this article contains supplemental material.

Abbreviations used in this article: ANA, anti-nuclear Ab; CHX, cycloheximide; Foxo1/3, Foxo1 and Foxo3; HA, hemagglutinin; *Mst1/2*, *Mst1* and *Mst2*; SP, single positive; Treg, regulatory T cell.

cancer cells (22). However, T cells from *Mst1*-deficient mice and human patients exhibit enhanced apoptosis (23–25) in addition to the mutant phenotypes of impaired adhesion and migration in mice (25–29), suggesting that *Mst1* may exert different cellular functions in tissue/cell type–specific manners (28). Both patients and mice with homozygous *Mst1*-null mutations display autoimmune manifestations (23, 24, 29), indicating critical roles of *Mst1* in autoimmune diseases. However, the mechanistic contribution of *Mst1/2* to disease remains elusive.

In this study we have identified *Mst1* as an important factor that promotes *Foxp3* expression and Treg development/function and simultaneously attenuates TCR-stimulated Akt activation. *Mst1* deficiency impairs *Foxp3* expression and Treg development/function owing to excessive degradation of Foxo1/3. Mechanistic study reveals that Mst1 enhances Foxo1/3 stability directly by phosphorylating Foxo1/3 and indirectly by antagonizing TCR-induced Akt activation; however, it does not seem to regulate Foxo1/3 cellular localization in T cells. Furthermore, we show that mutant phenotypes, such as overactivation of naive T cells, splenomegaly, and autoimmune pathological changes, in $Mst1^{-/-}$ mice are suppressed in the $Mst1^{-/-}$ bone marrow chimera by cotransplanted *wt* Tregs. Finally, we demonstrate that *Mst1/2* play a partially redundant role in Treg development. Therefore, our findings indicate that *Mst1/2* are important for controlling Treg development and preventing autoimmunity in mice, but also shed new light on our understanding of *Mst1* deficiency–mediated human immunodeficiency syndrome.

Materials and Methods

Mice

$Mst1^{-/-}$ mice and $Mst1^{fl/-}$*Lck-cre* were described previously (26). The generation of $Mst2^{-/-}$ mice is described in Supplemental Fig. 1. All mice except for B6.SJL and $Rag1^{-/-}$ from the Jackson Laboratory were maintained on a 129/Sv genetic background and raised in a specific pathogen–free facility. Experiments were conducted with consent from the Animal Care and Use Committee of the Institute of Developmental Biology and Molecular Medicine at Fudan University, Shanghai, China.

Plasmid and Abs

The *Foxo1*, *Foxo3*, and *Foxo3S207A* expression vectors and *Mst1* RNA interference (*shMst1*) plasmid were described previously (20, 21). The Foxo1S212A was generated by site-directed mutagenesis and verified by sequencing. The MIGR1-Flag-Foxo3 retrovirus vector was generated by cloning Flag-tagged-Foxo3 cDNA into MIGR1. The Foxp3 luciferase reporter plasmid was a gift from Yun-Cai Liu (La Jolla Institute for Allergy and Immunology, La Jolla, CA). Abs against the following proteins were used for our studies: CD4, CD8, CD44, CD62L, Foxp3, IL-2, IL-4, IFN-γ, and IL-17A (eBioscience); CD3, CD28, CD45.1, CD45.2, Smad2/3, NF-ATc1 (Becton Dickinson); B220, p-Smad3($Ser^{423/425}$), and p-Foxo1(S212)/Foxo3(S207) (Invitrogen); Creb, p-Creb(Ser^{133}), Foxo1, p-Foxo1(S256), p-Foxo1(Thr^{24}), Foxo3, Akt, p-Akt(S473), and p-Smad2($Ser^{465/467}$) (Cell Signaling); p-Ets-1(Thr^{38}), HA, and FLAG (Sigma); myc (SC-40), LaminB, and Actin (Santa Cruz); GAPDH (Beyotime).

Histology

Tissue processing and frozen section and immunofluorescent microscopic analysis were performed as described elsewhere (30). The analysis for infiltration foci was described previously (31).

Autoantibody detection and immunofluorescent microscopy

For the anti-nuclear Ab (ANA) test, Hep-2 cell and monkey liver cells (EUROIMMUN) were immunofluorescently stained with *wt* and $Mst1^{-/-}$ sera. For the extractable nuclear Ab test, an ENA kit (EUROIMMUN) was used according to the manufacturer's instructions. To analyze Foxo1/3 localization, fresh isolated peripheral lymphocytes (for Foxo1) or MIGR1-Flag-Foxo3–infected CD4 T cells (for Foxo3) were immunofluorescently stained with the appropriate Abs.

Cell purification and flow cytometry analysis

$CD4^+$ T cells and $CD4^+CD25^+$ Tregs were purified using the Mouse CD4 kit or $CD4^+CD25^+$ Treg cells kit (11461D, 11463D; Invitrogen). $CD4^+$ $CD25^-$ cells were purified by depleting $CD25^+$ cells with an anti-CD25/Anti-Rat IgG kit (11035; Invitrogen), followed by further purification using a Mouse CD4 kit. Intracellular FACS for Foxp3/cytokines was conducted using a kit (00-5523; eBioscience) or performed as described elsewhere (32). 7-Aminoactinomycin D (Sigma-Aldrich) was used to label dead cells. All samples were analyzed with a Calibur or a Cyan FACS machine and FlowJo software (TreeStar).

Retroviral transduction

293T cells were cotransfected with MIGR1-Flag-Foxo3 (or MIGR1) and pCL packaging plasmid using Lipofectamine 2000, and recombinant viruses were harvested 48 h later. Purified peripheral $CD4^+$ T cells were first stimulated with plate-bound anti-CD3 and soluble anti-CD28 for 48 h, then infected with retrovirus in the presence of 8 μg/ml polybrene by centrifuging cells at 1000 × *g* for 60 min at room temperature. At 48 h post infection, cells were collected for immunofluorescent staining.

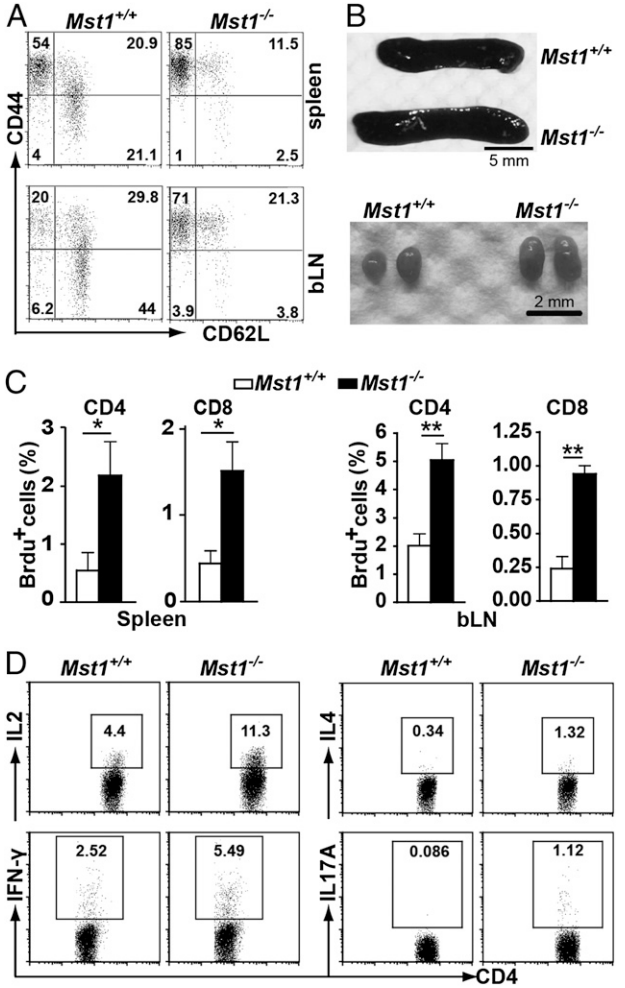

FIGURE 1. T cell activation and differentiation in $Mst1^{-/-}$ mice. (**A**) Flow cytometry analysis of the expression of CD44 and CD62L in CD4 T cells from spleen and brachial lymph node (bLN) of 1-y-old *wt* and $Mst1^{-/-}$ mice. Numbers in quadrants indicate percent of cells in each. (**B**) Representative gross anatomy of spleen (*upper panel*) and submandibular gland lymph node (*lower panel*) from *wt* and $Mst1^{-/-}$ mice at 1.5 y of age. (**C**) Quantification of BrdU incorporation in CD4 and CD8 T cells from spleen (*left two panels*) and bLN (*right two panels*) in *wt* and $Mst1^{-/-}$ mice. (**D**) Intracellular FACS analysis of the expression of IL-2, IL-4, IFN-γ, and IL-17 in splenic CD4 T cells from 8-wk-old *wt* and $Mst1^{-/-}$ mice after stimulation for 6 h with PMA and ionomycin. Data in (A), (B), and (D) are representative of at least three independent experiments. Values in (C) represent the means ± SEM of three separate experiments. $*p < 0.05$, $**p < 0.01$.

Quantitative PCR

Total RNA was extracted from purified peripheral CD4$^+$ T cells with TRIzol (Invitrogen). RT-PCR was carried out with TaKaRa RNA PCR Kit (AMV) according to the manufacturer's instructions. Quantitative PCR reactions were performed on Mx3000P (Stratagene) with the Fast SYBR Green QPCR Master Mix (Stratagene), and data were analyzed with MxPro software. Expression of *Gapdh* was used as internal control for real-time PCR. The primer sequences are as follows: Foxo1-F, 5′-AAGAGCGTGCCCTACTTCAAGG-3′; Foxo1-R, 5′-TCTTGCCTCCCTCTGGATTGAG-3′; Foxo3-F, 5′-AAACGGCTCACTTTGTCCCAG-3′; Foxo3-R, 5′-TCTTGCCCGTGCCTTCATTC-3′; Gapdh-L1, 5′-TGTTCCTACCCCCAATGTGTCC-3′; Gapdh-R1, 5′-GGAGTTGCTGTTGAAGTCGCAG-3′; Nr4a2-F, 5′-ATCATCAGAGGGTGGGCAGAGAAG-3′; Nr4a2-R, 5′-TGGGTTGGACCTGTATGCTAAGC-3′.

Treg suppression assay

A total of 6×10^4 splenic CD4$^+$CD25$^-$ cells labeled with CFSE (4) were cultured with mitomycin C–treated T cell–depleted splenocytes (4×10^4) and Con A (2 μg/ml) in the presence of 3×10^4 or 1.5×10^4 Tregs (spleen CD4$^+$25$^+$) for 72 h and then analyzed by FACS. The suppressive capacity of Tregs was calculated using the following formula: [100 × (1 − %CFSE^{low}CD4$^+$CD25$^-$ T cells in coculture/%CFSE^{low} CD4$^+$CD25$^-$ T cells alone)], as described previously (33).

In vitro Treg induction

Purified *wt* or *Mst1*$^{-/-}$ CD4$^+$CD25$^-$ splenic T cells (2×10^5) were cultured with 10 μg/ml plate-bound anti-CD3 plus 2 μg/ml soluble anti-CD28 Abs in the presence or absence of 1 or 5 ng/ml of recombinant human TGF-β (Peprotech) for 3 d. Foxp3$^+$ Tregs were quantified by intracellular FACS.

Generation and analysis of bone marrow chimeras

For the bone marrow chimera experiment, *Mst1*$^{-/-}$ mice were backcrossed to C57BL/6 for seven generations. Bone marrow cells (1×10^7) isolated from the femurs of *wt* or *Mst1*$^{-/-}$ mice were injected separately or coinjected (ratio wt:mutant = 1:4) into the tail vein of irradiated *Rag1*$^{-/-}$ (7 Gy) recipients. The congenic markers CD45.1 and CD45.2 were used to distinguish cells from different donors in the chimeras. Data were collected 6–7 wk later.

Adoptive transfer of Tregs

Spleen CD4$^+$CD25$^+$ Tregs were purified from the congenic CD45.1$^+$ C57BL/6 *wt* mice, and 3×10^5 CD45.1$^+$ *wt* Tregs were cotransplanted with the *Mst1*$^{-/-}$ bone marrow into the irradiated *Rag1*$^{-/-}$ (7 Gy) recipients. Then, 2 wk later, 3×10^5 *wt* Tregs were transferred into the same recipients through i.p. injection. The mice were sacrificed and analyzed 6–7 wk after bone marrow transplantation.

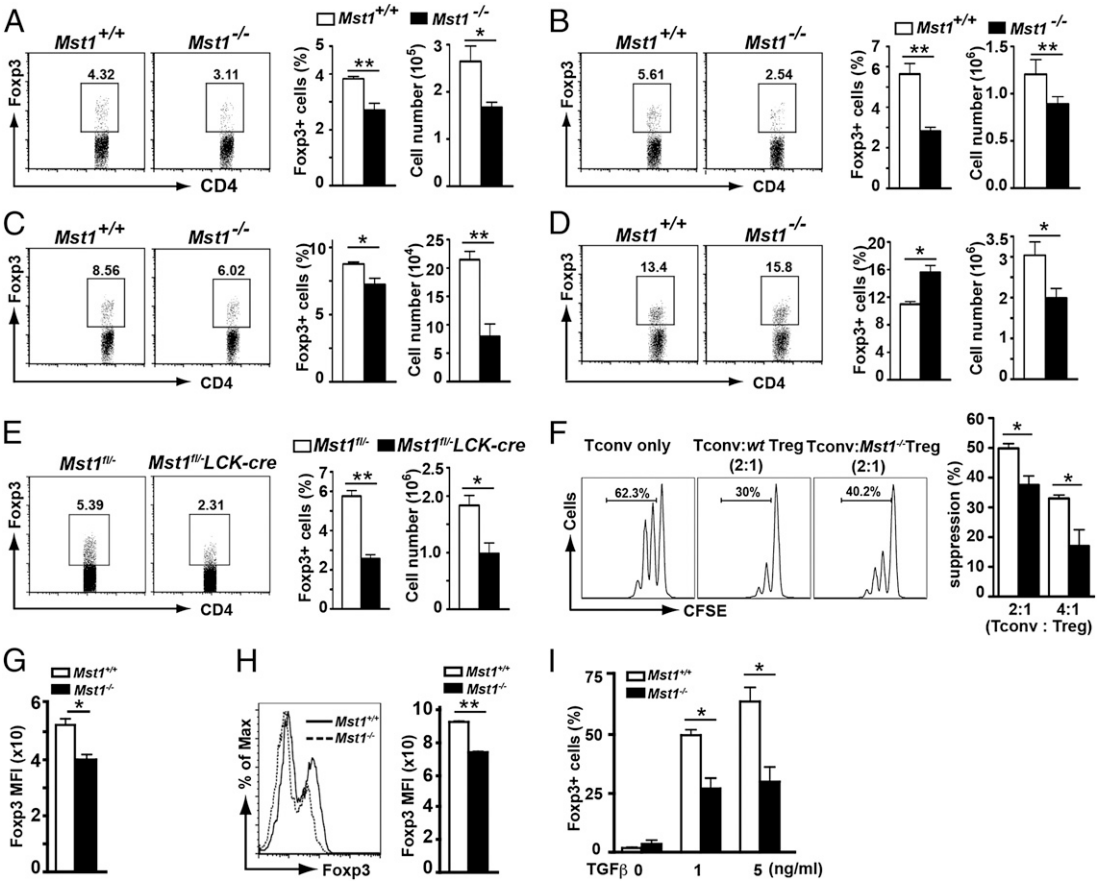

FIGURE 2. Impaired Foxp3 expression, development, and function of *Mst1*$^{-/-}$ Tregs. (**A**–**D**) Flow cytometry plots of Foxp3$^+$ CD4 SP cells in thymus [(A) and (B), *left panels*] and Foxp3$^+$ CD4 T cells in spleen [(C) and (D), *left panels*] from 1-wk-old [(A) and (C)] or 6- to 8-wk-old [(B) and (D)] *wt* and *Mst1*$^{-/-}$ mice, and frequency (*middle panel*) and number (*right panel*) of Tregs (at least four mice per group). (**E**) Flow cytometry plots of Foxp3$^+$CD4 SP in thymus of 6- to 8-wk-old *Mst1*$^{fl/-}$ and *Mst1*$^{fl/-}$*Lck-cre* mice, and frequency and number of Tregs ($n = 3$ mice per group). (**F**) Flow cytometry analysis of CFSE dilution in *wt* CD4$^+$CD25$^-$ T cells cultured alone or cocultured with *wt* or *Mst1*$^{-/-}$ CD4$^+$CD25$^+$ Tregs at a ratio of 2:1 (*left panels*) and suppression of *wt* CD4$^+$CD25$^-$ T cells by *wt* and *Mst1*$^{-/-}$ Tregs at a ratio of 2:1 and 4:1 (*right panels*). Numbers in *left panels* indicate the percentage of divided *wt* CD4$^+$CD25$^-$ T cells. (**G**) Quantification of Foxp3 expression in *wt* and *Mst1*$^{-/-}$ thymic Tregs, presented as mean fluorescence intensity (MFI) of *wt* and *Mst1*$^{-/-}$ Foxp3$^+$ CD4 SP thymocytes. (**H**) FACS analysis (*left panel*) and quantification (*right panel*) of Foxp3 expression in splenic CD4$^+$CD25$^-$ T cells stimulated with anti-CD3/anti-CD28 in the presence of 1 ng/ml of TGF-β for 3 d. (**I**) Foxp3$^+$ cells converted from *wt* or *Mst1*$^{-/-}$ splenic CD4$^+$CD25$^-$ T cells after stimulation with anti-CD3/anti-CD28 in the presence of indicated concentrations of TGF-β for 3 d. Numbers above outlined areas in left panels in (A)–(E) indicate percent of Foxp3$^+$ T cells in CD4$^+$ T cells. Data are from one representative of three independent experiments. Values in (A)–(F) (*right two panels*) and (G)–(I) represent the means ± SEM of three separate experiments. $^*p < 0.05$, $^{**}p < 0.01$.

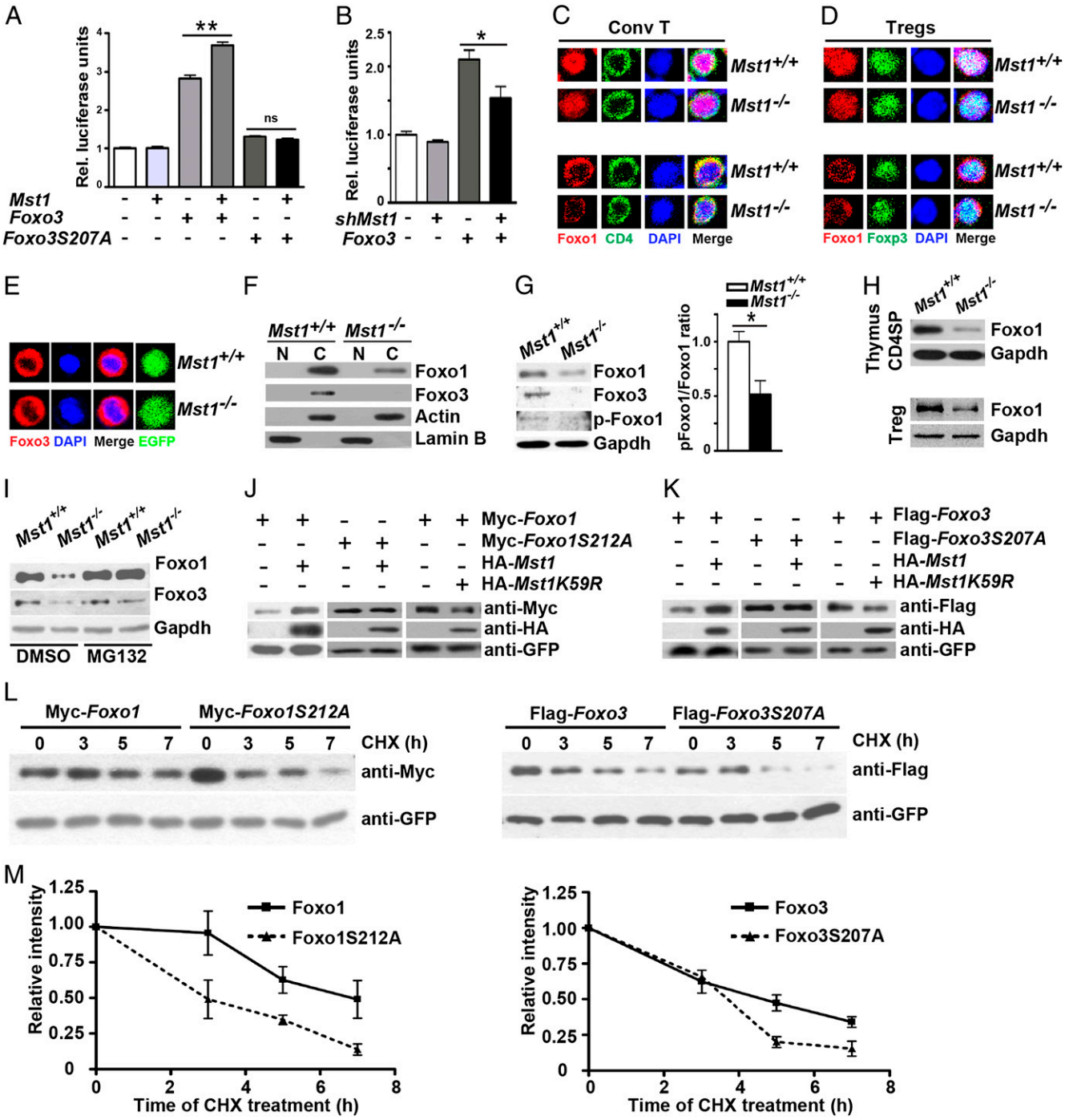

FIGURE 3. *Mst1* regulates *Foxp3* expression by modulating Foxo1/3 stability rather than affecting their subcellular location in CD4 T cells. (**A**) Quantification of luciferase activity in 293T cells transfected with a luciferase reporter plasmid containing the Foxp3 promoter together with an empty, *Mst1*, Foxo3, Foxo3S207, or both *Mst1* and Foxo3 or Foxo3S207 expression vectors. (**B**) Quantification of luciferase activity in Jurkat T cells electroporated with a luciferase reporter plasmid containing the Foxp3 promoter together with *Foxo3* expression and/or *shMst1* knockdown plasmids. (**C** and **D**) Representative immunofluorescence images of *wt* and *Mst1*$^{-/-}$ lymph node CD4 T cells (C) or Tregs (D) with nuclear (*upper panels*) or cytoplasmic Foxo1 (*lower panels*) after staining with the Abs indicated. (**E**) Representative immunofluorescence images of peripheral *wt* and *Mst1*$^{-/-}$ CD4 T cells expressing exogenous Flag-tagged Foxo3 stained with anti-Flag. (**F**) Western blot analysis for the distribution of endogenous Foxo1 and Foxo3 proteins after subcellular fractionation of peripheral CD4 T cells from *wt* and *Mst1*$^{-/-}$ mice. (**G**) Western blot analysis of Foxo1/3 and p-Foxo1/3 protein levels and densitometry quantification of p-Foxo1 and Foxo1 in splenic CD4 T cells freshly isolated from 6-wk-old *wt* and *Mst1*$^{-/-}$ mice. (**H**) Western blot analysis of Foxo1 in CD4 SP thymocytes (*upper panels*) and Tregs (*lower panels*) from *wt* and *Mst1*$^{-/-}$ mice. (**I**) Western blot analysis of Foxo1/3 of the CD4 T cells in (G) treated with 25 mM MG132 for 2 h in vitro after isolation. (**J**) Western blot analysis of exogenous Foxo1 and Foxo1S212A in 293T cells transfected with Myc-Foxo1 or Myc-Foxo1S212A expression plasmids together with GFP alone or with *Mst1*-HA or *Mst1*K59R-HA expression plasmids. (**K**) Experiments similar to those represented in (J) were performed for analysis of exogenous Foxo3 and Foxo3S207A. (**L**) The 293T cells were transfected with plasmids expressing Myc-Foxo1 or Myc-Foxo1S212A (*left*) or Flag-Foxo3 or Flag-Foxo3S207A (*right*) together with GFP and *Mst1*-HA expression plasmids. At 24 h (Foxo3/Foxo3S207A) or 48 h (Foxo1/Foxo1S212A) after transfection, the cells were treated with 50 μg/ml CHX for different periods, as indicated, followed by Western blot analysis with Abs as indicated. GFP was used for transfection efficiency control. (**M**) Quantitative analysis of Foxo1, Foxo1S212A, Foxo3, and Foxo3S207A proteins in (L). The density of each band was plotted against incubation time with the (*Figure legend continues*)

Luciferase-based reporter assay

The 293T cells were transfected with *Foxp3* promoter luciferase reporter plasmid together with *Foxo3*, *Mst1*, and *β-gal* expression vectors with Lipofectamine 2000. Jurkat T cells were transfected with empty, *shMst1*, or *Foxo3* expression plasmids separately, or *shMst1* and *Foxo3* expression plasmids together by electroporation, using a GENE PULSER II (Bio-Rad). Cells were collected 40 h after electroporation and analyzed as described previously (34).

Subcellular fractionation and immunoblotting

Cellular fractionation was performed according to the Nuclear Extraction Protocol (Invitrogen). Immunoblotting was performed as described previously (26), and images were collected with Tanon-5200 or by x-ray film exposure. For quantification of protein levels, appropriate film exposures were scanned and the density of bands was determined with Image J and normalized to band intensity for GAPDH or GFP.

Statistical analysis

Statistical analysis was conducted using an unpaired *t* test by GraphPad Prism 4. A p value < 0.05 was considered significant.

Results

Excessive activation and differentiation of T cells in Mst1$^{-/-}$ *mice*

Mst1 deficiency resulted in a slight but significant increase in the proportion of CD62L^{lo}CD44^{hi} effector T cells in secondary lymphoid organs of young (6–9 wk) *Mst1*$^{-/-}$ mice (25, 26). This phenotype was further enhanced (Fig. 1A), and splenomegaly and lymphadenopathy (Fig. 1B) were observed in aged *Mst1*$^{-/-}$ mice. BrdU pulse labeling experiments showed that the proliferation of *Mst1*$^{-/-}$ peripheral T cells was significantly enhanced (Fig. 1C). To determine whether *Mst1* deficiency affects T cell function, we evaluated the cytokine expression profile of *Mst1*$^{-/-}$ peripheral T cells. In comparison with their *wt* counterpart, a higher fraction of *Mst1*$^{-/-}$ splenic CD4 T cells produced effector cytokines such as IL-2, IL-4, IL-17, and IFN-γ after stimulation by PMA/ionomycin (Fig. 1D). These results suggest that *Mst1*$^{-/-}$ peripheral T cells are overactivated.

Mst1 *deficiency impairs the development and functions of Tregs*

Tregs are a subset of CD4 T cells that have an important responsibility in preventing the overactivation of other T cells and are essential in maintaining self-tolerance (35). To understand the cause of *Mst1*$^{-/-}$ T cell overactivation, we investigated whether *Mst1* deficiency affected Treg development. Our study showed that both the proportion and the number of Foxp3$^+$ CD4 single positive (SP) cells were significantly reduced in the thymus of young (1-wk-old) and adult *Mst1*$^{-/-}$ mice (Fig. 2A, 2B). These results demonstrate that *Mst1* is required for thymic Treg development.

Consistent with impaired thymic Treg development, the percentage and number of peripheral Foxp3$^+$ Tregs in 1-wk-old *Mst1*$^{-/-}$ mice decreased significantly (Fig. 2C). However, the proportion of peripheral Foxp3$^+$ Tregs in adult *Mst1*$^{-/-}$ mice was restored to a level similar to or even higher than that in the controls (Fig. 2D). Further study showed that a higher fraction of peripheral Tregs in adult *Mst1*$^{-/-}$ mice were labeled by BrdU (Supplemental Fig. 2A). Therefore, this enhanced proliferation, which could be a result of T cell homeostasis in adult *Mst1*$^{-/-}$ mice, may lead to an increase in the proportion of peripheral Tregs. Nonetheless, the total number of peripheral Tregs was still significantly lower than that in the controls (Fig. 2D), possibly owing to impaired T cell egress from the thymus (26) and/or impaired conversion of induced Tregs from peripheral T cells (Fig. 2I).

To further investigate whether *Mst1* regulates Treg development in a cell-intrinsic manner, we examined Treg development in the thymus of *Mst1*$^{fl/-}$*Lck-cre* mice. Our results showed that both the proportion and the number of Tregs in *Mst1*$^{fl/-}$*Lck-cre* mice were also significantly decreased (Fig. 2E).

Finally, we analyzed the function of *Mst1*$^{-/-}$ Tregs by performing an in vitro suppression assay. Results showed that *Mst1*$^{-/-}$ Tregs were less potent in suppressing the proliferation of naive T cells than were *wt* Tregs (Fig. 2F). Furthermore, we showed that *Mst1*-deficient bone marrow–mediated autoimmune pathological changes were rescued by *wt* Tregs, suggesting impaired suppression function of *Mst1*$^{-/-}$ Tregs in vivo. Taken together, our findings demonstrate that *Mst1* is required for the development and suppressive functions of Tregs.

Mst1 *deficiency impairs Foxp3 expression and Treg conversion from naive T cells induced by TGF-β*

To understand the mechanisms underlying the impaired development and function of *Mst1*$^{-/-}$ Tregs, we evaluated *Foxp3* expression, a hallmark of Tregs, by intracellular FACS analysis. The result revealed that *Foxp3* expression was reduced in *Mst1*$^{-/-}$ Tregs (Fig. 2G), suggesting that *Mst1* regulates Treg development by modulating *Foxp3* expression.

TGF-β is a prominent regulator for inducing Treg conversion from naive T cells via upregulating *Foxp3* expression (36). To further confirm *Mst1*-mediated regulation of *Foxp3* expression, we examined *Foxp3* induction and conversion in/of naive T cells with TGF-β/TCR costimulation. The results revealed that the mean fluorescence intensity of *Mst1*$^{-/-}$ Tregs stained with anti-Foxp3 was weaker than that of *wt* counterparts (Fig. 2H). Our analysis also showed that compared with *wt* counterparts, almost 2-fold fewer *Mst1*$^{-/-}$ CD4$^+$CD25$^-$ T cells were converted into Foxp3$^+$ Tregs when induced with TGF-β (Fig. 2I). These results indicate that *Mst1* is required for optimal *Foxp3* expression and Treg conversion from naive T cells.

Ablation of Mst1 *does not affect subcellular localization of Foxo1/3 in T cells*

Foxp3 transcription is coordinately regulated by multiple transcription factors, such as NFAT, CREB, Ets-1, Smad and Nr4a2, and Foxo 1/3 (37). However, our studies showed that *Mst1* deficiency had no effect on the phosphorylation of CREB, Ets-1, and Smads; nuclear entry of NFAT; and Nr4a2 mRNA level in peripheral T cells (Supplemental Fig. 2E–G). These results rule out the possibility that *Mst1* modulates *Foxp3* expression by affecting the transcriptional activities of these transcription factors.

Two transcription factors, Foxo1/3, are required for *Foxp3* expression and Treg development (4, 5). Mst1 phosphorylates Foxo1/3 and promotes their nuclear entry in fibroblasts and granule neurons (20, 21). Therefore, we assumed that Mst1 regulates *Foxp3* expression and Treg development by modulating subcellular localization of Foxo1/3. To verify our assumption, we first examined whether *Mst1* could enhance Foxo3-mediated Foxp3 expression. Our study showed that cotransfection with *Foxo3* and *Mst1* led to a significantly higher luciferase expression compared with the transfection with *Foxo3* only in 293T cells. We found that a S207A mutation in Foxo3 dramatically reduced its transcriptional activity

density at 0 h as 100%. All images and blots shown are representative of three experiments with similar results. Values in (A), (B), (G), and (M) represent the means ± SEM of three separate experiments. *$p < 0.05$, **$p < 0.01$. C, Cytoplasm; N, nuclear.

and cotransfection of *Mst1* with *Foxo3S207A* had no effect on transcriptional activities of Foxo3S207A (Fig. 3A). We also found that reducing the level of endogenous Mst1 protein by short hairpin RNA in Jurkat T cells resulted in a significant decrease of luciferase activity driven by *Foxp3* promoter (Fig. 3B, Supplemental Fig. 2B), further confirming the effect of *Mst1* on *Foxo3*-mediated *Foxp3* expression. These results demonstrate that *Mst1* modulates Foxo3-mediated *Foxp3* expression.

To further understand the molecular mechanisms by which *Mst1* regulates *Foxp3* expression, we evaluated the subcellular localization of Foxo1 proteins in peripheral $Mst1^{-/-}$ T cells and Tregs, respectively, by immunofluorescent staining. Surprisingly, we found that the percentages of $Mst1^{-/-}$ and *wt* peripheral CD4 T cells containing cytoplasmic Foxo1 were very similar (68.4% ± 3.4 and 68.8% ± 4,respectively) (Fig. 3C, Supplemental Fig. 2C). The percentage of $Mst1^{-/-}$ Tregs having cytoplasmic Foxo1 was also not significantly different from that of control Tregs, although many fewer Tregs contain cytoplasmic Foxo1 proteins (Fig. 3D, Supplemental Fig. 2C). Owing to unavailability of Foxo3 Abs for immunofluorescent staining, the subcellular localization of Foxo3 was examined in peripheral CD4 T cells transduced with *Foxo3*-expressing retrovirus, and 100% mutant and control peripheral T cells (n = 30, respectively) examined had cytoplasmic Foxo3 (Fig. 3E). To further confirm the above result, subcellular fractionation/Western blot analysis was performed. The study showed that the majority of Foxo1 and Foxo3 proteins were located in the cytoplasm in both $Mst1^{-/-}$ and *wt* peripheral CD4 T cells (Fig. 3F). These results demonstrate that *Mst1* deficiency does not affect the cellular distribution of Foxo1/3 proteins in peripheral CD4 T cells and Tregs.

Mst1 *regulates Foxo1/3 protein stability*

Our subcellular fractionation/Western blot analysis also revealed that protein levels of Foxo1/3 were dramatically reduced in $Mst1^{-/-}$ peripheral T cells, suggesting that *Mst1* deficiency may affect Foxo1/3 protein expression. Further Western blot analysis with whole-cell lysate also showed that both total protein level and the phosphorylation of Foxo1/3 in $Mst1^{-/-}$ peripheral CD4 T cells were dramatically reduced compared with these measures in controls (Fig. 3G). The reduction of Foxo1 protein level was also observed in $Mst1^{-/-}$ Tregs and thymic CD4 SP cells (Fig. 3H). These results confirm that *Mst1* is required for regulating Foxo1/3 protein expression.

To investigate the mechanisms underlying the regulation of Foxo1/3 expression, we quantified *Foxo1*/3 mRNAs in $Mst1^{-/-}$ and *wt* T cells. The *Foxo1*/3 mRNA levels in $Mst1^{-/-}$ T cell were found to be comparable to those in the *wt* controls (Supplemental Fig. 2D). Then, we asked if *Mst1* deficiency affects *Foxo1*/3 expression at the translational and/or posttranslational level. Results showed that *Foxo1*/3 protein levels in the $Mst1^{-/-}$ and *wt* control T cells were similar when the cells were treated with a proteasome inhibitor, MG132, to inhibit proteasome-dependent protein degradation (Fig. 3I). Furthermore, we found that Foxo1/3 protein levels were higher in 293T cells cotransfected with hemagglutinin (HA)–tagged *Mst1* (Fig. 3J, 3K, *left*). These experiments demonstrate that *Mst1* stabilizes Foxo1/3 proteins rather than regulates *Foxo1/3* expression at the transcriptional level in mouse T cells.

Mst1 stabilizes Foxo1 and Foxo3 proteins by phosphorylating S212 and S207, respectively

Foxo1/3 are degraded by proteasomes after Akt-mediated phosphorylation (8, 9). Because Mst1 can phosphorylate Foxo1 and Foxo3 at S212 and S207, respectively (20, 21), and the S207A mutation in Foxo3 abolished its transcriptional activity toward the *Foxp3* gene (Fig. 3A), we investigated whether phosphorylation by Mst1 is required for maintaining protein stability. The results showed that cotransfection of *Mst1* resulted in higher protein levels of Foxo1 and Foxo3, but had no effect on those of non–phosphorylation-mimic mutants, Foxo1S212A and Foxo3S207A (Fig. 3J, 3K, *middle*). Furthermore, cotransfection of *Mst1K59R*, a kinase-inactive form, did not enhance but instead reduced the expression of Foxo1/3 (Fig. 3J, 3K, *right*). These results demonstrate that Mst1 kinase activity is required to maintain the stability of Foxo1/3.

Finally, we confirmed the differential stability of the exogenous Foxo1 and Foxo1S212A in 293T cells treated with cycloheximide (CHX), which specifically inhibits protein synthesis. Foxo1S212A levels decreased dramatically after 3 h of CHX treatment, whereas Foxo1 remained unchanged at the same time point. (Fig. 3L, 3M, *left*). Similar results were also obtained for Foxo3 and Foxo3S207A (Fig. 3L, 3M, *right*). Taken together, these results strongly suggest that phosphorylation of Foxo1/3 by Mst1 is necessary for maintaining Foxo1/3 stability. Foxo1/3 degradation is one of the factors leading to impaired *Foxp3* expression in $Mst1^{-/-}$ Treg development.

Mst1 stabilizes Foxo1 and Foxo3 protein by inhibiting Akt activation

Foxp3 expression and Treg development require signaling from TCR. Both Mst1 and Akt can be activated by TCR stimulation (38, 39). However, constitutively activated Akt inhibits *Foxp3* expression and Treg development (10). Because Mst1 and Akt

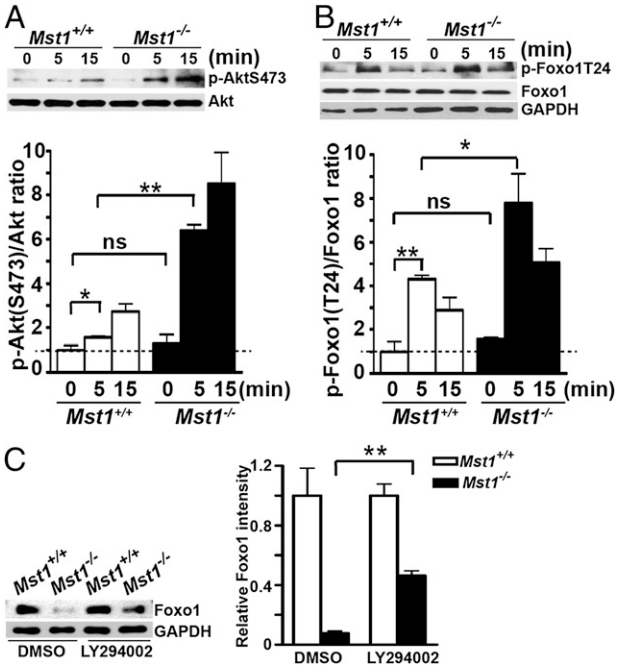

FIGURE 4. Overactivation of Akt in $Mst1^{-/-}$ peripheral CD4 T cells. (**A** and **B**) Western blot analyses and densitometry quantification of the phosphorylation of Akt (S473) (A) and phosphorylation of Foxo1(T24) (B) in *wt* and $Mst1^{-/-}$ peripheral CD4 T cells stimulated with TCR (anti-CD3/anti-CD28) for the indicated times. For ease of comparing Foxo1 phosphorylation, a similar level of Foxo1 protein was loaded for the $Mst1^{-/-}$ cell lysate and the control in (B). (**C**) Western blot (*left panel*) and quantitative (*right panel*) analysis of Foxo1 protein level in *wt* and $Mst1^{-/-}$ peripheral CD4 T cells stimulated with anti-CD3/anti-CD28 for 2 h in the presence of Ly294002 (15 μM) or DMSO. Blots shown are representative of three experiments with similar results. Values in (A)–(C) represent the means ± SEM of three separate experiments. *$p < 0.05$, **$p < 0.01$.

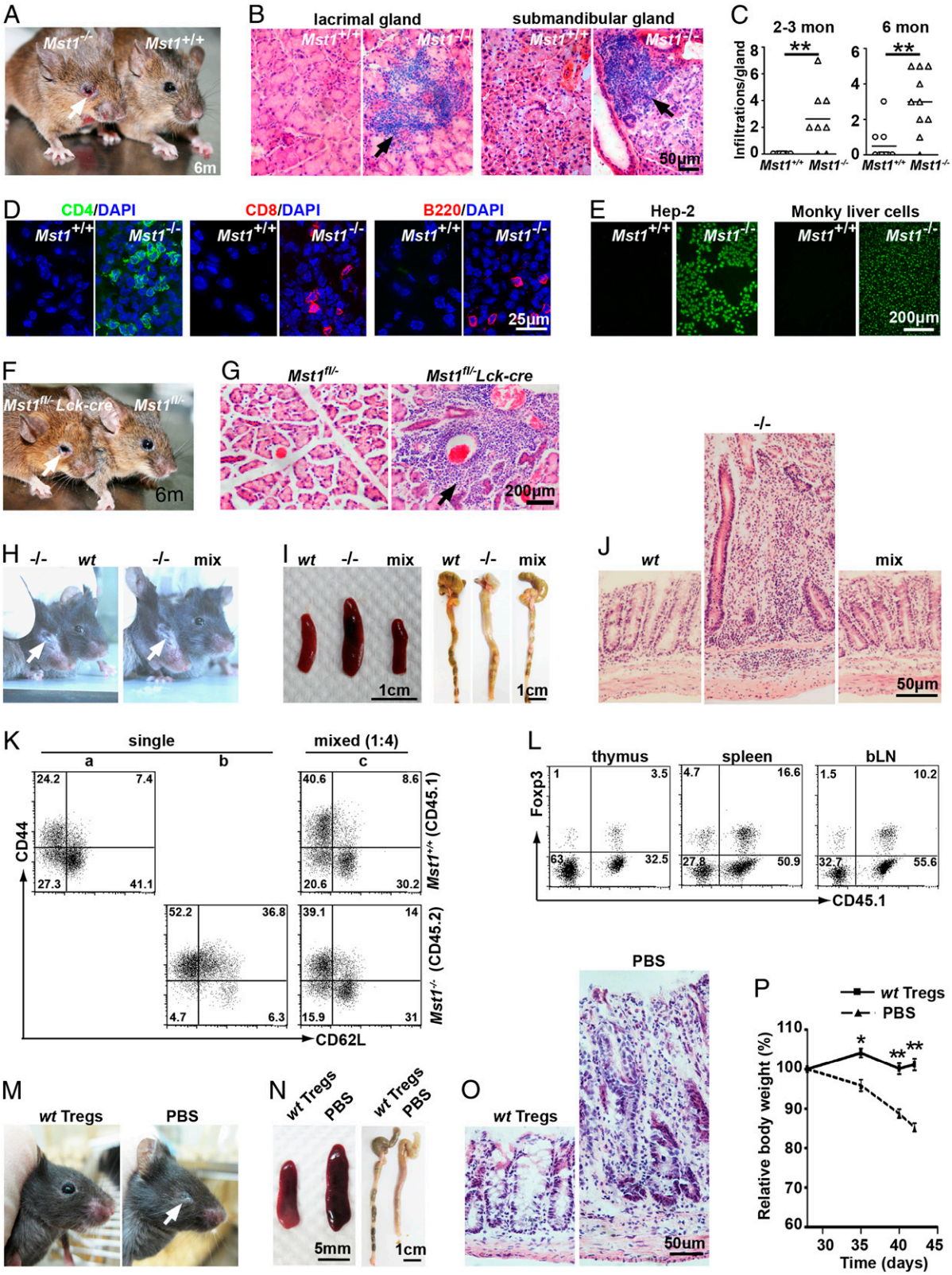

FIGURE 5. *Mst1* deficiency–mediated autoimmunity/inflammation in mice. (**A**) The *wt* and *Mst1*$^{-/-}$ mice at 6 mo of age. (**B**) H&E staining of sections of lacrimal (2 mo) and submandibular (6 mo) glands of *wt* and *Mst1*$^{-/-}$ mice. (**C**) Quantification of infiltration in lacrimal glands from mice of indicated genotypes and ages. (**D**) Immunofluorescence staining of frozen sections of lacrimal glands from 6-mo-old mice of indicated genotypes with anti-CD4, -CD8, and -B220, respectively. (**E**) Immunofluorescence photomicrograph of commercial slides stained with sera from *wt* and *Mst1*$^{-/-}$ mice for the ANA test. (**F**) The *Mst1*$^{fl/-}$ and *Mst1*$^{fl/-}$*Lck-cre* mice at 6 mo of age. (**G**) Photomicrograph of H&E-stained section of lacrimal glands from the mice in (F). (**H**–**J**) Development of immune pathological changes in the *Mst1*$^{-/-}$ or *wt* or *wt*/*Mst1*$^{-/-}$ mixed chimera 6–7 wk after transplantation. Representative photograph of the chimeric mice (H), spleens and colons (I), and H&E-stained colon sections (J) from the mice in (H). (**K**) Flow cytometry of effector (CD44^{hi}CD62L^{lo}) and naive (CD44^{lo}CD62L^{hi}) CD4 T cells in the brachial lymph node from sublethally irradiated *Rag1*$^{-/-}$ mice 6–7 wk after transplantation with (**a**) *wt* (CD45.1), (**b**) *Mst1*$^{-/-}$ (CD45.2), or (**c**) *wt*/*Mst1*$^{-/-}$ mixed (1:4) bone marrows. (**L**) Flow cytometry of Tregs (Foxp3^{+}) in (*Figure legend continues*)

proteins interact and inhibit reciprocally in cancer cells (22) and activated Akt also destabilizes Foxo1/3 (8), we hypothesized that Mst1 may also maintain Foxo1/3 stability through inhibiting TCR-induced Akt activation. To test this possibility, we examined the activation status of Akt in $Mst1^{-/-}$ peripheral CD4 T cells after TCR stimulation. Our results showed that Akt was more activated in $Mst1^{-/-}$ T cells than in the controls upon TCR stimulation (Fig. 4A). To further confirm the effect of *Mst1* deficiency–mediated overactivation of Akt on Foxo1/3 proteins, we evaluated the Akt-specific phosphorylation of Foxo1. Our study showed that phosphorylation of Foxo1 at T24 was significantly increased in $Mst1^{-/-}$ CD4 T cells after TCR stimulation (Fig. 4B). Finally, we demonstrated that inhibiting Akt activity could partially rescue *Mst1* deficiency–mediated degradation of the Foxo1 protein (Fig. 4C). All these results suggest that *Mst1* may promote *Foxp3* expression and Treg development by inhibiting Akt activation in mice.

Mst1-*deficient mice are prone to autoimmune disease*

Genetic abnormalities that affect Tregs cause or predispose to autoimmunity (40). Consistent with the mutant phenotypes of impaired development/function of $Mst1^{-/-}$ Tregs and overactivation of peripheral $Mst1^{-/-}$ T cells, *Mst1*-deficient mice were found to be prone to autoimmune disease. *Mst1*-deficient mice tended to develop skin lesions around the eyes as early as 2 mo of age. These abnormalities became much more severe as the mice aged (Fig. 5A, Supplemental Fig. 3A, Table I). The infiltrations of mononuclear cells were detected in the lacrimal and submandibular glands of $Mst1^{-/-}$ mice at the age of 2 and 6 mo, respectively (Fig. 5B, 5C), and in other tissues such as lung and liver at the age of 1 y (Supplemental Fig. 3B). The number of infiltration foci increased as the mice aged (Fig. 5C, Supplemental Fig. 3C), and both CD4/CD8 T cells and B cells were easily detected in the infiltrated areas (Fig. 5D). We also found that the circulating ANA, a critical marker for autoimmunity, was present in 78% (7/9) of sera of half-year-old $Mst1^{-/-}$ mice, but were absent in the control group (Fig. 5E). In addition, an ENA test demonstrated that anti-nucleosome and anti-dsDNA Abs were present in 100% and 43%, respectively, of ANA-positive $Mst1^{-/-}$ sera (Table II). Collectively, our data demonstrate that $Mst1^{-/-}$ mice are prone to developing autoimmune disease.

Next we further investigated whether *Mst1*-deficient T cells were sufficient to cause autoimmune diseases in mice. Our study showed that $Mst1^{fl/-}$*Lck-cre* mice (26), in which *Mst1* is specifically deleted in T cells, developed skin lesions around the eyes and infiltration of mononuclear cells in the lacrimal gland at a lower frequency and later ages compared with $Mst1^{-/-}$ mice (Fig. 5F, 5G, Supplemental Fig. 3D). These results demonstrate a T cell–intrinsic role of *Mst1* in protecting mice from autoimmune disease.

Mst1-*deficient cell-mediated autoimmunity/inflammation in* $Rag1^{-/-}$ *mice can be suppressed by* wt *Tregs*

To further confirm the role of *Mst1*-deficient cells in autoimmunity, we evaluated the ability of *Mst1*-deficient cells to induce autoimmunity or inflammation by generating $Mst1^{-/-}$ (CD45.2), *wt* (CD45.1), or $Mst1^{-/-}$/*wt* mixed bone marrow chimeric mice, respectively. Our studies showed that skin lesions around eyes and splenomegaly observed in $Mst1^{-/-}$ mice were observed only in $Mst1^{-/-}$ chimera, but not in mixed or *wt* chimera (Fig. 5H, 5I). Furthermore, we found that $Mst1^{-/-}$ chimera exhibited severe colitis, which was observed neither in mixed chimera nor in unmanipulated 1-y-old *Mst1*-deficient mice (Fig. 5I, 5J). Next, we determined whether *wt* cells from bone marrow would suppress the activation of $Mst1^{-/-}$ naive T cells. The results revealed that the majority of peripheral T cells in the $Mst1^{-/-}$ chimera were activated ($CD44^{hi}CD62L^{lo}$) effector T cells (Fig. 5K*b*, Supplemental Fig. 3E). In contrast, the proportion of activated peripheral $Mst1^{-/-}$ T cells in the recipients of $Mst1^{-/-}$/*wt* mixed chimera was similar (in brachial lymph nodes) to that of *wt* counterparts (Fig. 5K*c*, Supplemental Fig. 3E) or dramatically reduced (in spleen, Supplemental Fig. 3G, 3H). These results strongly suggest that autoimmunity or inflammation induced by *Mst1*-deficient cells and activation of peripheral $Mst1^{-/-}$ T is not due to an intrinsic defect or defects of effector T cells but can be suppressed by the presence of *wt* cells from the bone marrow cotransplanted.

Table I. Skin lesions in *wt* and $Mst1^{-/-}$ mice

Genotype	2–5 mo, %	6–9 mo, %	>10 mo, %
wt	0 (0/19)	0 (0/12)	0 (0/9)
$Mst1^{-/-}$	23.1 (6/26)	36.4 (4/11)	78.8 (26/33)

We also analyze the development of $Mst1^{-/-}$ Tregs in mixed chimera. FACS analysis showed that the proportion of $Mst1^{-/-}$ thymic Tregs ($FoxP3^{+}CD45.1^{-}$) was ~ 7.5-fold lower than that of the *wt* counterpart ($FoxP3^{+}CD45.1^{+}$) in mixed chimera, although the majority of thymic $CD4^{+}$ SP cells ($FoxP3^{-}CD45.1^{-}$) were from $Mst1^{-/-}$ bone marrow (Fig. 5L, Supplemental Fig. 3F). Consistent with the impaired thymic $Mst1^{-/-}$ Treg development, the proportion of $Mst1^{-/-}$ peripheral Tregs was also ~ 2- to 3.5-fold lower than that of the *wt* control in peripheral lymphoid organs of the mixed chimera (Fig. 5L, Supplemental Fig. 3F). These results demonstrate that $Mst1^{-/-}$ bone marrow contributes much less than the coinjected *wt* counterpart to thymic Tregs in mixed chimera and further confirm the intrinsic functions of *Mst1* in Treg development.

Tregs suppress excessive immune responses and are critical for maintaining dominant tolerance. Because the development of $Mst1^{-/-}$ Tregs was impaired in both *Mst1*-deficient mice (Fig. 2A–D) and $Mst1^{-/-}$/*wt* mixed chimera (Fig. 5L) and because *wt* cells differentiating from *wt* bone marrow suppressed autoimmunity/inflammation in the chimera (Fig. 5H–J), we hypothesized that the autoimmune disease in $Mst1^{-/-}$ chimera was due to the abnormality of $Mst1^{-/-}$ Tregs. To test this hypothesis, *wt* Tregs were transferred into $Mst1^{-/-}$ bone marrow–reconstituted $Rag1^{-/-}$ mice, and inflammation and peripheral T cell activation status were analyzed 6–7 wk later. Our results showed that transplantation of *wt* Tregs rescued autoimmune pathological changes, including skin lesions around the eyes, colitis, and body weight loss, and suppressed the activation of peripheral T cells and

thymus, spleen, and brachial lymphoid of the *wt*/$Mst1^{-/-}$ mixed chimera in (Kc). (**M–P**) Development of immune pathological changes in the sublethally irradiated $Rag1^{-/-}$ mice 6–7 wk after transplantation with $Mst1^{-/-}$ bone marrow in the presence or absence of adoptive transferred *wt* Tregs. Representative photograph of the mice (M), spleens and colons (N), and H&E-stained colon sections (O) from the mice in (M). (P) Statistical analysis of body weight of the chimeric mice in (M). The body weight of each mouse at 28 d after bone marrow transplantation was defined as 100%. $n = 3$ for each group. Images and flow cytometry plots shown are representative of at least three experiments with similar results. White and black arrows [in (A), (B), (F), (G), (H), and (M)] indicate skin lesions around the eyes and mononuclear cell infiltration, respectively. Each dot in (C) represents an individual mouse. Values in (C) and (P) represent the means ± SEM. *wt*, −/−, or mix represent *wt*, $Mst1^{-/-}$, or *wt*/$Mst1^{-/-}$ mixed chimera, respectively. $*p < 0.05$, $**p < 0.01$.

Table II. Spectrum of anti-nuclear Abs

Ag	Genotype		Ag	Genotype	
	wt	*Mst1*$^{-/-}$		*wt*	*Mst1*$^{-/-}$, %
nRNP	—	—	Jo-1	—	—
Sm	—	—	CENP B	—	—
SSA	—	—	dsDNA	—	43 (3/7)
SSB	—	—	Nucleosome	—	100 (7/7)
Ro-52	—	—	Histone	—	—
Scl-70	—	—	Rib-P	—	—

—, Not detected in 7 *wt* or *Mst1*$^{-/-}$ mice.

splenomegaly of the *Mst1*$^{-/-}$ chimera (Fig. 5M–P, Supplemental Fig. 3I, 3J).

Altogether, the results above strongly suggest that abnormality of *Mst1*$^{-/-}$ Tregs is the main cause of autoimmunity in *Mst1*-deficient mice.

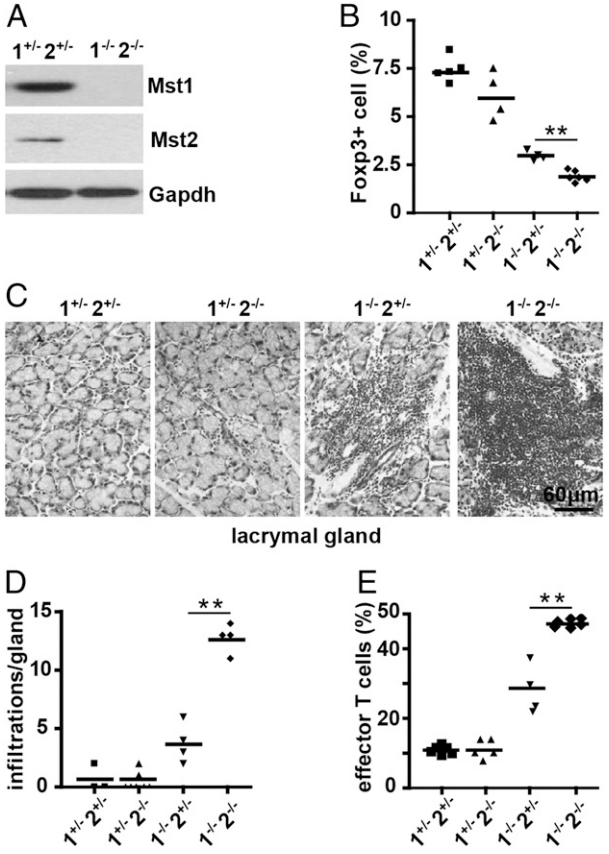

FIGURE 6. Redundancy of *Mst1* and *Mst2* in Treg development. (**A**) Western blot analysis of protein expression of Mst1 and Mst2 in *Mst1*$^{+/fl}$ *Mst2*$^{+/-}$*Lck-cre* and *Mst1*$^{fl/-}$*Mst2*$^{-/-}$*Lck-cre* mice. Blots shown are representative of three experiments with similar results. (**B**) Scatter plot showing the mean frequency of thymic Tregs (Foxp3^{+} CD4 SP cells) in the thymus of 6- to 8-wk-old mice of the indicated genotypes. (**C** and **D**) Representative microscopic images of H&E staining of lacrimal gland sections (C) and scatter plot showing the mean number of infiltration foci per gland (D) from 6-mo-old mice of the indicated genotypes. (**E**) Scatter plot showing the mean frequency of effector (CD44^{hi}CD62^{lo}) T cells in the spleen from 6- to 8-wk-old mice of the indicated genotypes. Each dot in the scatter plots represents an individual mouse. $n \geq 4$ mice for each genotype. Data are representative of three independent experiments. $1^{+/-}2^{+/-}$, $1^{+/-}2^{-/-}$, $1^{-/-}2^{+/-}$, and $1^{-/-}2^{-/-}$ represent *Mst1*$^{+/fl}$*Mst2*$^{+/-}$*Lck-cre, Mst1*$^{+/fl}$*Mst2*$^{-/-}$*Lck-cre, Mst1*$^{fl/-}$*Mst2*$^{+/-}$*Lck-cre*, and *Mst1*$^{fl/-}$*Mst2*$^{-/-}$*Lck-cre* mice, respectively. $^{**}p < 0.01$.

Redundant functions of Mst1 and Mst2 in Treg development

Mouse Mst1/2 proteins share 76% identical amino acids and are functionally redundant for embryonic development and tumorigenesis (15, 16, 41). *Mst1*$^{-/-}$ mice displayed compromised development and functions of Tregs and inflammatory autoimmune disease (Figs. 2, 5), but *Mst2*$^{-/-}$ mice did not (Supplemental Fig. 1E and data not shown). These results suggest that *Mst1* plays more important roles in regulating Treg development and autoimmune pathological changes than does *Mst2,* but it does not rule out the possibility that *Mst1/2* function redundantly in these processes. To test this possibility, we generated *Mst1*$^{fl/-}$*Mst2*$^{-/-}$*Lck-cre* mice in which both *Mst1/2* were deleted in T cells (Fig. 6A). Further analysis revealed that *Mst2* did have redundant roles in the control of Treg development and immunopathological changes. We found that deleting one allele each in *Mst1* and *Mst2* genes had no effect on the proportion of thymic Tregs, but deleting one allele of *Mst1* and two alleles of *Mst2* resulted in a substantial reduction in the proportion of thymic Tregs (Fig. 6B). This effect is more prominent when the proportions of thymic Tregs in *Mst1*$^{fl/-}$*Mst2*$^{-/-}$ *Lck-cre* and *Mst1*$^{fl/-}$*Mst2*$^{+/-}$*Lck-cre* mice were compared (Fig. 6B). Our findings demonstrate a redundant function for *Mst1/2* in the control of thymic Treg development.

Histological analyses revealed more severe lymphocyte infiltration in lacrimal glands in *Mst1*$^{fl/-}$*Mst2*$^{-/-}$*Lck-cre* mice than in *Mst1*$^{fl/-}$*Mst2*$^{+/-}$*Lck-cre* mice, in addition to skin lesions around the eyes in *Mst1*$^{fl/-}$*Mst2*$^{-/-}$*Lck-cre* and *Mst1*$^{fl/-}$*Mst2*$^{+/-}$*Lck-cre* mice (Fig. 6C, 6D). FACS analysis showed that the percentages of activated peripheral T cells (CD44^{hi}CD62L^{lo}) from *Mst1*$^{fl/+}$*Mst2*$^{+/-}$ *Lck-cre* and *Mst1*$^{fl/+}$*Mst2*$^{-/-}$*Lck-cre* mice were very similar (Fig. 6E), suggesting that *Mst1* plays a major role in controlling the activation of peripheral T cells. However, 47.52% ± 0.75 of peripheral CD4 T cells became activated T cells in *Mst1*$^{fl/-}$*Mst2*$^{-/-}$ *Lck-cre* mice, whereas only 28.13% ± 5.04 were activated T cells in *Mst1*$^{fl/-}$*Mst2*$^{+/-}$*Lck-cre* mice (Fig. 6E), strongly suggesting that *Mst1/2* also plays a redundant role in the control of activation of peripheral T cells.

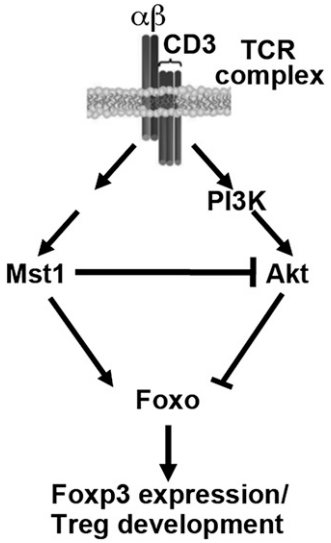

FIGURE 7. Proposed model by which *Mst1* regulates *Foxp3* expression and Treg development through maintaining Foxo activity in direct and indirect ways. TCR/CD28 stimulation simultaneously activates *Mst1* and the *PI3K–Akt* pathway. Mst1 can attenuate TCR-induced Akt activation to reduce Akt-mediated degradation of Foxo1/3. At the same time, Mst1 can phosphorylate Foxo1/3 to enhance their stabilities. Thus, *Mst1* ensures the Foxo1/3 protein stability and activity required for *Foxp3* expression and Treg development.

In summary, our findings demonstrate that *Mst1/2* play partially redundant roles in the control of thymic Treg development and immunopathological changes, and also suggest that the role of *Mst1* is more dominant than that of *Mst2*. Given the function redundancy of *Mst1* and *Mst2* mentioned earlier, it is conceivable to postulate that *Mst1* and *Mst2* may share a similar mechanism in regulation of Treg development and immunopathology (Fig 7).

Discussion

In this report, we demonstrate that *Mst1* regulates Foxp3 expression and Treg development/function by enhancing the stability of Foxo1/3 proteins through phosphorylating Foxo1/3 and attenuating Akt activation. Previous studies reported that *Mst1* regulated Foxo activity by phosphorylating Foxo proteins and promoting their nuclear accumulation in nonhematopoietic cells (20, 21). However, we found that *Mst1* deficiency did not significantly change the localization of Foxo proteins, but rather led to their excessive degradation in thymic CD4 SP cells, peripheral T cells, and Tregs. Lower levels of Foxo proteins were also observed in *Mst1*-deficient human PBMCs and peripheral T cells of mice from one laboratory (23, 24, 42), but the underlying mechanisms are unknown. In this article, we demonstrate that *Mst1* regulates Foxo1/3 stability through phosphorylation in the lymphoid T cells and that excessive degradation of Foxo proteins impairs *Foxp3* induction and Treg development in $Mst1^{-/-}$ mice. Our findings not only support the idea that *Mst/hpo* exerts its various cellular functions by regulating different downstream targets in tissue- and/or cell type–specific manners (28), but also uncovers a new mechanism by which *Mst1* regulates Foxo signaling.

TCR/CD28 stimulation is required for Foxp3 expression and Treg development, but also activates the PI3K–Akt pathway, which inhibits de novo Foxp3 expression and Treg development. To explain this paradoxical phenomenon, it has been proposed that undefined factors specifically attenuate TCR/CD28-induced Akt activation and therefore maintain Foxo proteins in activating status to induce Foxp3 expression (37). In this article, we have, to our knowledge, for the first time identified *Mst1* as one of such long-searched-for factors. *Mst1* can be activated by TCR/CD28 stimulation in T cells (25, 38). We have found that *Mst1* deficiency not only results in destabilization of Foxo1/3 proteins but also increases Akt activation in peripheral T cells. On the basis of these results, we propose that upon TCR/CD28 stimulation, activated Mst1 maintains sufficient Foxo activity required for Foxp3 expression and Treg development by directly or indirectly stabilizing Foxo proteins through phosphorylation and inhibition of TCR/CD28-induced Akt activation (Fig. 7). Because Mst1 and Akt are reciprocally inhibitory (22, 43), it is conceivable that they may repress each other to orchestrate the fine balance of TCR signals needed to regulate Foxp3 expression and Treg development.

Foxo1 has been demonstrated to be a pivotal regulator of Treg function (44). In this article, we have demonstrated that *Mst1* deficiency dramatically reduces the protein level of Foxo1 (Fig. 3H) in $Mst1^{-/-}$ Tregs. Thus, it seems likely that *Mst1* deficiency–mediated reduction of Foxo1 proteins could be one explanation for impaired suppressive function of $Mst1^{-/-}$ Tregs. *Mst1* regulates LFA-1 activation (38). Because $LFA\text{-}1^{-/-}$ Tregs also show suppressive defects in vivo and in vitro, it is possible that reduction of the suppressive function of $Mst1^{-/-}$ Tregs is in part due to *Mst1* deficiency–mediated inability to activate LFA-1 integrin. During the revision of this manuscript, Tomiyama et al. (45) have reported that $Mst1^{-/-}$ Tregs display defective suppressor function and are impaired in their interactions with Ag-presenting dendritic cells owing to inefficient formation of an immunological synapse via LFA-1/ICAM-1 (45). However, the effect of *Mst1* deficiency on Treg development seems unlikely to be a secondary effect of impaired LFA-1 integrin activation because the mutant Treg phenotype of *Mst1*-deficient mice is different from that of *LFA-1* deficiency. $LFA\text{-}1^{-/-}$ mice have a reduced frequency of Tregs in peripheral lymphoid organs but an increased frequency of Tregs in the thymus. In contrast, $Mst1^{-/-}$ mice exhibit a reduced number of Tregs in both the thymus and the periphery. The reduction of Foxo1/3 proteins in $Mst1^{-/-}$ thymic CD4 SP cells (Fig. 3H) may account for the impaired Treg development in the thymus.

Human *Mst1* deficiency leads to a novel primary immunodeficiency syndrome including autoimmune manifestations (23, 24). Ueda et al. (29) also reported autoimmune disease in aged (1-y-old) *Mst1*-deficient mice. In this study, we found that some novel and severe autoimmune phenotypes, such as skin lesions around the eyes, could be detected in our $Mst1^{-/-}$ mice as early as 2 mo of age, in addition to the lymphocyte infiltration in the multiple organs of aged mutant mice. This discrepancy could have resulted because different strains of mice were used for the studies. It has been implied that impaired thymocyte selection was responsible for autoimmune disease in $Mst1^{-/-}$ mice (29). However, we showed in this article that excessive T cell activation, splenomegaly, and immune disease manifestations, including skin lesions around the eyes and severe colitis, were observed only in $Mst1^{-/-}$ chimera, but not in the $Mst1^{-/-}$/*wt* mixed chimera. Our study demonstrates that *Mst1* deficiency–mediated autoimmunity or inflammation can be suppressed by the presence of *wt* cells derived from cotransplanted bone marrow, therefore suggesting that autoimmunity in $Mst1^{-/-}$ mice may not be intrinsic to $Mst1^{-/-}$ effector T cells. Indeed, all autoimmune pathology phenotypes, activation of peripheral T cells, and splenomegaly of the $Mst1^{-/-}$ chimera were rescued by cotransplanted *wt* Tregs (Fig. 5M–P, Supplemental Fig. 3I, 3J). This result strongly suggests that loss of dominant tolerance mediated by Tregs in $Mst1^{-/-}$ mice is the main reason leading to T cell activation and probably autoimmunity phenotypes. Our findings that all *Mst1* deficiency–mediated autoimmunity or inflammation can be suppressed by the presence of *wt* cells from mixed bone marrow or cotransplanted *wt* Tregs may provide help in designing a strategy to cure immunodeficiency syndrome in *Mst1*-deficient patients.

Acknowledgments

We thank Dr. Yun-Cai Liu for the Foxp3-luciferase reporter plasmid, Dr. Xiaohui Wu for scientific discussion, and Alan Yu for the editing of English.

Disclosures

The authors have no financial conflicts of interest.

References

1. Ziegler, S. F. 2006. FOXP3: of mice and men. *Annu. Rev. Immunol.* 24: 209–226.
2. Ono, M., H. Yaguchi, N. Ohkura, I. Kitabayashi, Y. Nagamura, T. Nomura, Y. Miyachi, T. Tsukada, and S. Sakaguchi. 2007. Foxp3 controls regulatory T-cell function by interacting with AML1/Runx1. *Nature* 446: 685–689.
3. Allan, S. E., A. N. Alstad, N. Merindol, N. K. Crellin, M. Amendola, R. Bacchetta, L. Naldini, M. G. Roncarolo, H. Soudeyns, and M. K. Levings. 2008. Generation of potent and stable human CD4+ T regulatory cells by activation-independent expression of FOXP3. *Mol. Ther.* 16: 194–202.
4. Harada, Y., Y. Harada, C. Elly, G. Ying, J. H. Paik, R. A. DePinho, and Y. C. Liu. 2010. Transcription factors Foxo3a and Foxo1 couple the E3 ligase Cbl-b to the induction of Foxp3 expression in induced regulatory T cells. *J. Exp. Med.* 207: 1381–1391.
5. Ouyang, W., O. Beckett, Q. Ma, J. H. Paik, R. A. DePinho, and M. O. Li. 2010. Foxo proteins cooperatively control the differentiation of Foxp3+ regulatory T cells. *Nat. Immunol.* 11: 618–627.
6. Kerdiles, Y. M., E. L. Stone, D. R. Beisner, M. A. McGargill, I. L. Ch'en, C. Stockmann, C. D. Katayama, and S. M. Hedrick. 2010. Foxo transcription factors control regulatory T cell development and function. *Immunity* 33: 890–904.
7. Brunet, A., A. Bonni, M. J. Zigmond, M. Z. Lin, P. Juo, L. S. Hu, M. J. Anderson, K. C. Arden, J. Blenis, and M. E. Greenberg. 1999. Akt pro-

motes cell survival by phosphorylating and inhibiting a Forkhead transcription factor. *Cell* 96: 857–868.
8. Huang, H., K. M. Regan, F. Wang, D. Wang, D. I. Smith, J. M. van Deursen, and D. J. Tindall. 2005. Skp2 inhibits FOXO1 in tumor suppression through ubiquitin-mediated degradation. *Proc. Natl. Acad. Sci. USA* 102: 1649–1654.
9. Matsuzaki, H., H. Daitoku, M. Hatta, K. Tanaka, and A. Fukamizu. 2003. Insulin-induced phosphorylation of FKHR (Foxo1) targets to proteasomal degradation. *Proc. Natl. Acad. Sci. USA* 100: 11285–11290.
10. Haxhinasto, S., D. Mathis, and C. Benoist. 2008. The AKT-mTOR axis regulates de novo differentiation of CD4+Foxp3+ cells. *J. Exp. Med.* 205: 565–574.
11. Merkenschlager, M., and H. von Boehmer. 2010. PI3 kinase signalling blocks Foxp3 expression by sequestering Foxo factors. *J. Exp. Med.* 207: 1347–1350.
12. Fruman, D. A., and G. Bismuth. 2009. Fine tuning the immune response with PI3K. *Immunol. Rev.* 228: 253–272.
13. Zeng, Q., and W. Hong. 2008. The emerging role of the hippo pathway in cell contact inhibition, organ size control, and cancer development in mammals. *Cancer Cell* 13: 188–192.
14. Zhou, D., C. Conrad, F. Xia, J. S. Park, B. Payer, Y. Yin, G. Y. Lauwers, W. Thasler, J. T. Lee, J. Avruch, and N. Bardeesy. 2009. Mst1 and Mst2 maintain hepatocyte quiescence and suppress hepatocellular carcinoma development through inactivation of the Yap1 oncogene. *Cancer Cell* 16: 425–438.
15. Lu, L., Y. Li, S. M. Kim, W. Bossuyt, P. Liu, Q. Qiu, Y. Wang, G. Halder, M. J. Finegold, J. S. Lee, and R. L. Johnson. 2010. Hippo signaling is a potent in vivo growth and tumor suppressor pathway in the mammalian liver. *Proc. Natl. Acad. Sci. USA* 107: 1437–1442.
16. Song, H., K. K. Mak, L. Topol, K. Yun, J. Hu, L. Garrett, Y. Chen, O. Park, J. Chang, R. M. Simpson, et al. 2010. Mammalian Mst1 and Mst2 kinases play essential roles in organ size control and tumor suppression. *Proc. Natl. Acad. Sci. USA* 107: 1431–1436.
17. Zhou, D., Y. Zhang, H. Wu, E. Barry, Y. Yin, E. Lawrence, D. Dawson, J. E. Willis, S. D. Markowitz, F. D. Camargo, and J. Avruch. 2011. Mst1 and Mst2 protein kinases restrain intestinal stem cell proliferation and colonic tumorigenesis by inhibition of Yes-associated protein (Yap) overabundance. *Proc. Natl. Acad. Sci. USA* 108: E1312–E1320.
18. Kim, T. S., D. H. Lee, S. K. Kim, S. Y. Shin, E. J. Seo, and D. S. Lim. 2012. Mammalian sterile 20-like kinase 1 suppresses lymphoma development by promoting faithful chromosome segregation. *Cancer Res.* 72: 5386–5395.
19. Cheung, W. L., K. Ajiro, K. Samejima, M. Kloc, P. Cheung, C. A. Mizzen, A. Beeser, L. D. Etkin, J. Chernoff, W. C. Earnshaw, and C. D. Allis. 2003. Apoptotic phosphorylation of histone H2B is mediated by mammalian sterile twenty kinase. *Cell* 113: 507–517.
20. Lehtinen, M. K., Z. Yuan, P. R. Boag, Y. Yang, J. Villén, E. B. Becker, S. DiBacco, N. de la Iglesia, S. Gygi, T. K. Blackwell, and A. Bonni. 2006. A conserved MST-FOXO signaling pathway mediates oxidative-stress responses and extends life span. *Cell* 125: 987–1001.
21. Yuan, Z., M. K. Lehtinen, P. Merlo, J. Villén, S. Gygi, and A. Bonni. 2009. Regulation of neuronal cell death by MST1-FOXO1 signaling. *J. Biol. Chem.* 284: 11285–11292.
22. Cinar, B., P. K. Fang, M. Lutchman, D. Di Vizio, R. M. Adam, N. Pavlova, M. A. Rubin, P. C. Yelick, and M. R. Freeman. 2007. The pro-apoptotic kinase Mst1 and its caspase cleavage products are direct inhibitors of Akt1. *EMBO J.* 26: 4523–4534.
23. Abdollahpour, H., G. Appaswamy, D. Kotlarz, J. Diestelhorst, R. Beier, A. A. Schäffer, E. M. Gertz, A. Schambach, H. H. Kreipe, D. Pfeifer, et al. 2012. The phenotype of human STK4 deficiency. *Blood* 119: 3450–3457.
24. Nehme, N. T., J. Pachlopnik Schmid, F. Debeurme, I. André-Schmutz, A. Lim, P. Nitschke, F. Rieux-Laucat, P. Lutz, C. Picard, N. Mahlaoui, et al. 2012. MST1 mutations in autosomal recessive primary immunodeficiency characterized by defective naive T-cell survival. *Blood* 119: 3458–3468.
25. Zhou, D., B. D. Medoff, L. Chen, L. Li, X. F. Zhang, M. Praskova, M. Liu, A. Landry, R. S. Blumberg, V. A. Boussiotis, et al. 2008. The Nore1B/Mst1 complex restrains antigen receptor-induced proliferation of naïve T cells. *Proc. Natl. Acad. Sci. USA* 105: 20321–20326.
26. Dong, Y., X. Du, J. Ye, M. Han, T. Xu, Y. Zhuang, and W. Tao. 2009. A cell-intrinsic role for Mst1 in regulating thymocyte egress. *J. Immunol.* 183: 3865–3872.
27. Katagiri, K., T. Katakai, Y. Ebisuno, Y. Ueda, T. Okada, and T. Kinashi. 2009. Mst1 controls lymphocyte trafficking and interstitial motility within lymph nodes. *EMBO J.* 28: 1319–1331.
28. Mou, F., M. Praskova, F. Xia, D. Van Buren, H. Hock, J. Avruch, and D. Zhou. 2012. The Mst1 and Mst2 kinases control activation of rho family GTPases and thymic egress of mature thymocytes. *J. Exp. Med.* 209: 741–759.
29. Ueda, Y., K. Katagiri, T. Tomiyama, K. Yasuda, K. Habiro, T. Katakai, S. Ikehara, M. Matsumoto, and T. Kinashi. 2012. Mst1 regulates integrin-dependent thymocyte trafficking and antigen recognition in the thymus. *Nat. Commun.* 3: 1098.
30. Peng, C., J. Ye, S. Yan, S. Kong, Y. Shen, C. Li, Q. Li, Y. Zheng, K. Deng, T. Xu, and W. Tao. 2012. Ablation of vacuole protein sorting 18 (Vps18) gene leads to neurodegeneration and impaired neuronal migration by disrupting multiple vesicle transport pathways to lysosomes. *J. Biol. Chem.* 287: 32861–32873.
31. Li, H., M. Dai, and Y. Zhuang. 2004. A T cell intrinsic role of Id3 in a mouse model for primary Sjogren's syndrome. *Immunity* 21: 551–560.
32. Vanvalkenburgh, J., D. I. Albu, C. Bapanpally, S. Casanova, D. Califano, D. M. Jones, L. Ignatowicz, S. Kawamoto, S. Fagarasan, N. A. Jenkins, et al. 2011. Critical role of Bcl11b in suppressor function of T regulatory cells and prevention of inflammatory bowel disease. *J. Exp. Med.* 208: 2069–2081.
33. Venken, K., M. Thewissen, N. Hellings, V. Somers, K. Hensen, J. L. Rummens, and P. Stinissen. 2007. A CFSE based assay for measuring CD4+CD25+ regulatory T cell mediated suppression of auto-antigen specific and polyclonal T cell responses. *J. Immunol. Methods* 322: 1–11.
34. Yan, S., I. M. Berquin, B. R. Troen, and B. F. Sloane. 2000. Transcription of human cathepsin B is mediated by Sp1 and Ets family factors in glioma. *DNA Cell Biol.* 19: 79–91.
35. Bäckdahl, L., A. Bushell, and S. Beck. 2009. Inflammatory signalling as mediator of epigenetic modulation in tissue-specific chronic inflammation. *Int. J. Biochem. Cell Biol.* 41: 176–184.
36. Chen, W., W. Jin, N. Hardegen, K. J. Lei, L. Li, N. Marinos, G. McGrady, and S. M. Wahl. 2003. Conversion of peripheral CD4+CD25− naive T cells to CD4+CD25+ regulatory T cells by TGF-beta induction of transcription factor Foxp3. *J. Exp. Med.* 198: 1875–1886.
37. Ouyang, W., and M. O. Li. 2011. Foxo: in command of T lymphocyte homeostasis and tolerance. *Trends Immunol.* 32: 26–33.
38. Katagiri, K., M. Imamura, and T. Kinashi. 2006. Spatiotemporal regulation of the kinase Mst1 by binding protein RAPL is critical for lymphocyte polarity and adhesion. *Nat. Immunol.* 7: 919–928.
39. Deane, J. A., and D. A. Fruman. 2004. Phosphoinositide 3-kinase: diverse roles in immune cell activation. *Annu. Rev. Immunol.* 22: 563–598.
40. Wing, K., and S. Sakaguchi. 2010. Regulatory T cells exert checks and balances on self tolerance and autoimmunity. *Nat. Immunol.* 11: 7–13.
41. Oh, S., D. Lee, T. Kim, T. S. Kim, H. J. Oh, C. Y. Hwang, Y. Y. Kong, K. S. Kwon, and D. S. Lim. 2009. Crucial role for Mst1 and Mst2 kinases in early embryonic development of the mouse. *Mol. Cell. Biol.* 29: 6309–6320.
42. Choi, J., S. Oh, D. Lee, H. J. Oh, J. Y. Park, S. B. Lee, and D. S. Lim. 2009. Mst1-FoxO signaling protects naïve T lymphocytes from cellular oxidative stress in mice. *PLoS ONE* 4: e8011.
43. Yuan, Z., D. Kim, S. Shu, J. Wu, J. Guo, L. Xiao, S. Kaneko, D. Coppola, and J. Q. Cheng. 2010. Phosphoinositide 3-kinase/Akt inhibits MST1-mediated pro-apoptotic signaling through phosphorylation of threonine 120. *J. Biol. Chem.* 285: 3815–3824.
44. Ouyang, W., W. Liao, C. T. Luo, N. Yin, M. Huse, M. V. Kim, M. Peng, P. Chan, Q. Ma, Y. Mo, et al. 2012. Novel Foxo1-dependent transcriptional programs control T(reg) cell function. *Nature* 491: 554–559.
45. Tomiyama, T., Y. Ueda, T. Katakai, N. Kondo, K. Okazaki, and T. Kinashi. 2013. Antigen-specific suppression and immunological synapse formation by regulatory T cells require the mst1 kinase. *PLoS ONE* 8: e73874.